PCCP

Accepted Manuscript

ROYAL SOCIETY OF CHEMISTRY

www.rsc.org/pccp

PCCP

RSCPublishing

ARTICLE

Mode-specific fragmentation of amino acid-containing clusters

Cite this: DOI: 10.1039/x0xx00000x

W. Scott Hopkins,[1,]* Rick A. Marta,[1] Vincent Steinmetz,[2] Terry B. McMahon[1,]**

Received 17th June 2015,
Accepted xxth XXX 2015

DOI: 10.1039/x0xx00000x

www.rsc.org/

A combination of infrared multiple photon dissociation (IRMPD) spectroscopy and density functional theory calculations have been employed to study the structures and mode−specific dissociation pathways of the proton-bound dimer of 3-trifluoromethylphenylalanine (3-CF_3-Phe) and trimethylamine (TMA). Three structural motifs are identified: canonical (charge-solvated), zwitterionic (charge-separated), and TMA-bridged. In the 1000 – 1350 cm^{-1} region, similar spectra are observed in the TMA•H^+ and 3-CF_3-Phe•H^+ product channels. At wavenumbers above 1350 cm^{-1}, infrared excitation of charge-solvated structures leads *exclusively* to production of protonated TMA, while excitation of zwitterionic or TMA-bridged structures results *exclusively* in production of protonated 3-CF_3-Phe. The cluster potential energy landscape is topologically mapped and mechanisms for isomerization and mode−selective dissociation are proposed. In particular, cluster transparency as a result of IR-induced isomerization is implicated in deactivation of some IRMPD channels.

Introduction

Amino acids that are isolated in the gas phase exhibit canonical, charge-solvated structures quite unlike the zwitterion (i.e., charge-separated) forms that they adopt in aqueous solution.[1-8] The only known exception to this generalized behaviour is arginine, which has been proposed to adopt a non-traditional zwitterion gas phase structure wherein the guanidine side chain acts as the proton accepting site.[2] It has therefore been a long-time goal of gas phase ion chemistry to identify the factors / conditions that lead amino acids to adopt the common solution phase structures. Previous work has shown that clustering with a single solvent molecule can stabilize the otherwise unfavourable zwitterion charge separation in isolated cationized amino acids.[1] In particular, alkylated amines seem to be especially good in this regard due to gas phase basicities (GBs) that are similar to those of amino acids.[6, 7, 9] For example, the GBs of phenylalanine and trimethylamine are 889 kJ•mol^{-1} and 918 kJ•mol^{-1}, respectively.[10] Consequently, the intermolecular proton sharing interaction between the protonated alkylamine and the amino acid carbonyl group stabilizes a similar intramolecular proton sharing / transfer between the amino acid OH and NH_2 groups.

The structures of gas phase amino acid clusters are typically determined using infrared vibrational spectroscopy. Spectroscopic investigations of these clusters are, however, challenging owing to the large number of possible isomeric structures.[9] Spectral complexity can be mitigated to some degree by employing low temperature sources (*e.g.*, supersonic expansion, electrospray ionization) to cool the clusters rotationally and vibrationally. However, if isomerization barriers are sufficiently high, a variety of conformational structures can be "frozen out" in production.[5, 9] Indeed, conformational trapping has been observed in systems with interconversion barriers as low as *ca.* 4.8 kJ•mol^{-1} (400 cm^{-1}).[11] It is therefore necessary that a thorough search of the cluster potential energy surface (PES) be undertaken to identify all isomers that are potential spectral carriers.

Recently, we reported on a combined experimental and computational study of proton-bound 3-cyanophenylalanine (3-CN-Phe) and trimethylamine (TMA) clusters.[9] In this work, an infrared multiple photon dissociation (IRMPD) spectroscopic study was supported by a detailed basin-hopping PES search and density functional theory (DFT) study. We found that the protonated 3-CN-Phe•TMA spectrum could be attributed to three structural motifs: (1) canonical, (2) zwitterion, and (3) TMA−bridged. Figure 1 provides a schematic depiction of these structural motifs. Moreover, each motif exhibited isomer-specific dissociation pathways. Canonical cluster species were found to exclusively produce TMA•H^+, zwitterion species fragmentation exclusively produced 3-CN-Phe•H^+, and the bridged structures accessed both thresholds with approximately

equal probability. Here we report a parallel series of experiments in which we studied the analogous 3-trifluoromethylphenylalanine (3-CF_3-Phe) cluster. We present a combined experimental and computational study of the protonated dimer of 3-CF_3-Phe and TMA to address the generality of TMA for stabilizing gas phase zwitterions and the mode-selective chemistry that is observed in the unimolecular decomposition.[12-17]

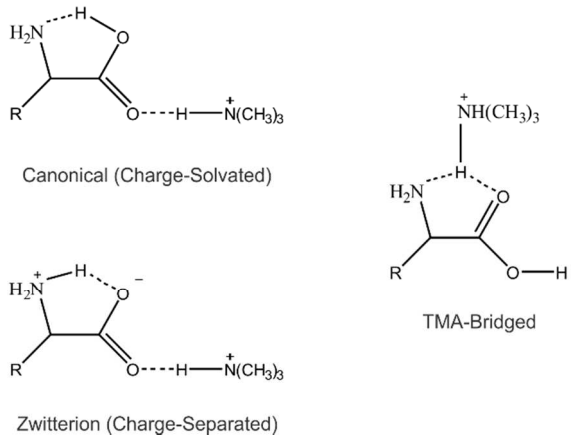

Figure 1. The general canonical, zwitterionic, and TMA-bridged structural motifs observed for protonated clusters of amino acids with trimethylamine.

Experimental

IRMPD spectra were recorded at the Centre de Laser Infrarouge d'Orsay (CLIO) free electron laser (FEL) facility at the University of Paris XI.[18] A detailed description of the experimental apparatus is available in references [19-22]. Aqueous solutions of approximately 50 μmol concentration were prepared from stoichiometric quantities of TMA hydrochloride (Sigma Aldrich) and 3-CF_3-Phe (Alpha Aesar). Chemicals were used without further purification. Positive mode electrospray ionization, ESI(+), was used to generate gas phase proton-bound 3-CF_3-Phe•TMA clusters. Nascent clusters were transferred to an ion trap mass spectrometer (Bruker Esquire 3000+) where they were mass-selected and subsequently irradiated by the tuneable output of the FEL over the 1000 – 2000 cm^{-1} range. Vibrational spectra were generated by monitoring parent ion signal depletions and daughter ion signal enhancements as a function of FEL wavenumber.

Computational Methods

A custom-written basin-hopping routine interfaced with the Gaussian 09 suite for computational chemistry was employed for structural sampling of protonated 3-CF_3-Phe•TMA.[23, 24] The protonated dimer was initially modelled using the AMBER force field, which was amended to include partial charges for the TMA and 3-CF_3-Phe moieties that were calculated at the B3LYP/6-31+G(d,p) level using the CHelpG partition scheme In total, *ca*. 40,000 protonated 3-CF_3-Phe•TMA cluster structures were sampled by the basin-hopping routine, resulting in the identification of 226 cluster isomers as determined by unique energies and geometries. Convergence criteria for the search were set to the default criteria of Gaussian 09.[23] This entire test set of unique isomer structures was then carried forward for treatment at the PM6 semi-empirical level of theory to refine cluster geometries, from which unique isomers were carried forward for treatment at the B3LYP/6-311++G(d,p) DFT level of theory.[25-28] This method resulted in identification of 26 unique proton-bound 3-CF_3-Phe•TMA cluster isomers within 60 kJ•mol^{-1} of the calculated ground state. To ensure that each isomer was a local minimum on the PES, normal mode analyses were undertaken. Calculated harmonic frequencies also served to predict the vibrational spectrum for each isomer. For selected isomers (*vide infra*), anharmonically corrected vibrational frequencies were also calculated.

Transition states were identified in two ways: with the basin-hopping treatment and with manual STQN searches that were associated with rotation of all dihedral angles of the saturated carbon chain and all proton transfer coordinates for the identified cluster minima.[29, 30] Each unique transition state (based on energy and geometry) was then distorted along the positive and negative directions of the unbound normal mode coordinate and re-optimized to determine the connected minima. Computational details, DFT results and cluster *XYZ* coordinates are provided in the Supporting Information.

Results and Discussion

Cluster Structures

The proton-bound dimer of 3-CF_3-Phe and TMA undergoes IRMPD via two mass channels: production of the neutral amino acid and protonated TMA (TMA•H^+; *m/z* = 60 amu), or the protonated amino acid and neutral TMA (3-CF_3-Phe•H^+; *m/z* = 234 amu). Interestingly, different IRMPD spectra are observed in each of the two mass channels for protonated 3-CF_3-Phe•TMA. The IRMPD spectra that were recorded by monitoring the 3-CF_3-Phe•H^+ and TMA•H^+ mass channels are shown in figures 2A and 2B, respectively. While only a single peak is observed in the carbonyl stretch region for TMA•H^+ production, two different peaks are observed in the C=O stretching region for the 3-CF_3-Phe•H^+ product mass channel. Since protonated 3-CF_3-Phe•TMA contains only one carbonyl moiety, the observation of three carbonyl peaks suggests that there are at least three isomeric forms of the cluster present in the sample for the given experimental conditions.

In examining the results of our computational study, an interesting picture emerges. Three cluster structural motifs are identified: (1) canonical, (2) zwitterion, and (3) species in which TMA•H^+ is oriented in a bridging fashion to the amine and carbonyl groups of the amino acid. Perhaps unsurprisingly, these are the same three structural motifs that were identified for the proton-bound dimer of 3-CN-Phe and TMA.[9] The calculated harmonic spectrum for the lowest energy member of each motif is shown in figures 2C-E. Since application of a scaling factor was not needed for spectral interpretation, unscaled harmonic wavenumbers are reported. Figure 3 shows

the lowest energy isomers of protonated 3-CF_3-Phe•TMA for each structural motif, namely, the canonical global minimum (isomer 1; 0.0 kJ•mol^{-1}), the first higher energy zwitterion cluster (isomer 7; 13.8 kJ•mol^{-1}), and the first higher energy TMA−bridged structure (isomer 12; 24.4 kJ•mol^{-1}). Note that isomers are numbered based on their energies relative to the global minimum (i.e., canonical isomers 2 – 6 have relative energies that are less than 13.8 kJ•mol^{-1}). At much higher energies, slight variations on the canonical, zwitterion, and TMA−bridged structural themes were observed (see Supporting Information), but these structures are likely unimportant with regard to the observed photochemistry.

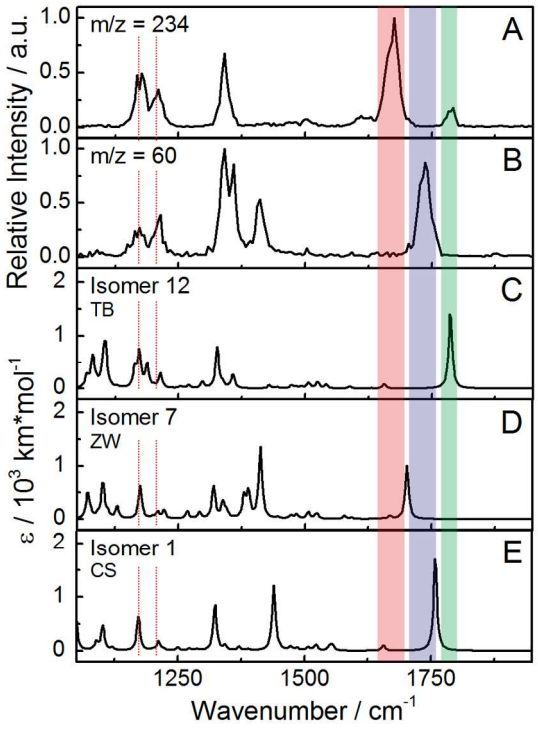

Figure 2. (A) IRMPD spectrum observed in the 3-CF_3-Phe•H^+ (*m/z* = 234 amu) mass channel. (B) IRMPD spectrum observed in the TMA•H^+ (*m/z* = 60 amu) mass channel. Predicted unscaled harmonic vibrational spectra for (C) the lowest energy TMA−bridged isomer at 24.4 kJ•mol^{-1}, (D) the lowest energy zwitterionic isomer at 13.8 kJ•mol^{-1} and, (E) the global minimum canonical isomer at 0.0 kJ•mol^{-1}. Calculations employed the B3LYP functional and 6-311++G(d,p) basis set.

Having assigned the spectral carriers based on the carbonyl stretching modes, the remaining bands can be assigned to specific vibrational modes associated with the three observed structural motifs. Details of spectral assignments are provided in the supporting information. The region from 1300 – 1425 cm^{-1} exhibits vibrational transitions associated with amine and hydroxyl functional groups. Note that three peaks are observed in the TMA•H^+ product channel spectrum (1332 cm^{-1}, 1350 cm^{-1}, and 1418 cm^{-1}) whereas only the 1332 cm^{-1} peak leads to production of 3-CF_3-Phe•H^+. Comparison with the calculated vibrational spectra suggest that the peak at 1418 cm^{-1} is associated with the COH bending motion of the charge solvated structures, while the peak at 1332 cm^{-1} is associated with the NH_3 umbrella mode in the zwitterion isomers. Observation of these modes is clear evidence that the hydrogen nuclei associated with the proton transfer coordinates are localized.

Both product mass channels exhibit broad features at 1210 cm^{-1} and 1235 cm^{-1}. In comparing the observed spectra (Figures 2A-B) to calculation (Figures 2C-E), we see that the experimental data appear to be a convolution of all three structural motifs. While the vibrational modes that contribute to these bands have relatively small calculated absorption cross sections, they are associated with motions along proton-transfer coordinates, which consistently exhibit intense IRMPD signals across the spectral region studied and in the analogous 3-cyanophenylalanine cluster.[9] It is therefore tempting to conclude that these modes are particularly active in IRMPD owing to efficient coupling with the dissociative threshold leading to TMA•H^+ and/or 3-CF_3-Phe•H^+ production. Parneix *et al.* have, however, shown that such a view may be too simplistic and that dynamic energy flow during the IRMPD process should be considered to properly model observed IRMPD intensities.[31] These same considerations also provide a reasonable explanation for the IRMPD phenomenon whereby predicted (usually weak) transitions are not observed experimentally.[9, 20-22, 32-36]

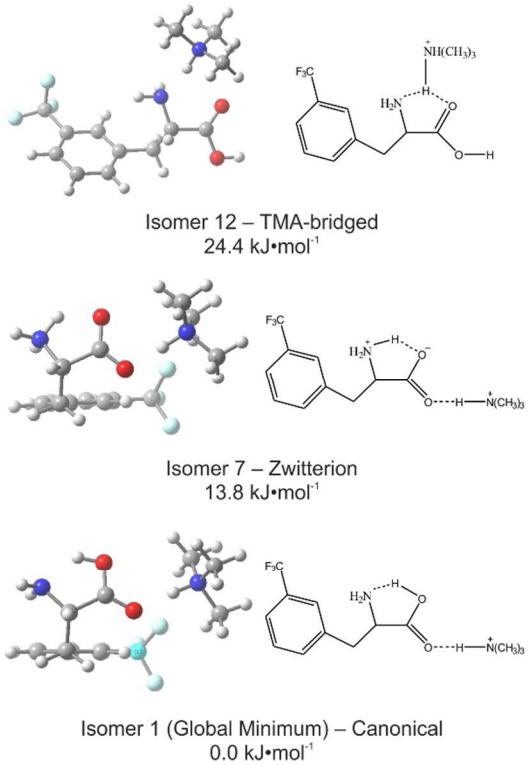

Figure 3. The global minimum (isomer 1), first higher energy zwitterionic (isomer 7) and first higher energy TMA−bridged (isomer 12) structures of protonated 3-CF_3-Phe•TMA. Standard Gibb's energies are reported. Calculations employed the B3LYP functional and 6-311++G(d,p) basis set.

Cluster Dynamics

The low energy region of the PES for protonated 3-CF_3-Phe•TMA was topologically mapped using the basin-hopping

algorithm.[37] To refine structures and relative energies, stationary points were then re-optimized at the B3LYP/6-311++G(d,p) level of theory. The B3LYP/6-311++G(d,p) method has previously been demonstrated to reliably model similar systems,[9, 38] and DFT results from these calculations accord well with analogous calculations at the MP2/*aug*-cc-pVTZ level of theory (*vide infra*). The topological map of protonated 3-CF_3-Phe•TMA is shown as a disconnectivity graph in figure 3,[37, 39] where the bottom of vertical lines correspond with local minima on the electronic PES and points where lines intersect correspond to energies above which minima can interconvert. Note that these connection points are not necessarily transition states, but energies at which barriers for isomer interconversion are overcome. Here, we use a coarse-grain energy sampling at increments of 25 kJ•mol^{-1}. By employing such a coarse-grained topologically mapping it is possible to identify funnel-like features on the PES. In the case of protonated 3-CF_3-Phe•TMA two major funnels are observed: one associated with the canonical and zwitterion structures, and a secondary funnel associated with the TMA-bridged isomers. Energy landscapes that exhibit multiple funnels usually also exhibit a separation of time scales for relaxation to funnel bottoms and relaxation to the true global minimum.[39] This accords well with the fact that TMA-bridged structures are observed experimentally, despite the fact that they are more than 24 kJ•mol^{-1} above the global minimum. Note also that each funnel exhibits a "willow tree" pattern, which generally corresponds with systems where relaxation to the funnel bottom is relatively slow.[39] In other words, the PES topological map suggests that several isomeric structures should be present in the ensemble that was probed with IRMPD. Again, this accords well with experiment; both canonical and zwitterion isomers were observed experimentally, and vibrational band widths of *ca.* 40 cm^{-1} are significantly larger than the typical CLIO FEL bandwidth of 25 cm^{-1}, thus suggesting the presence of multiple closely related isomers.[40]

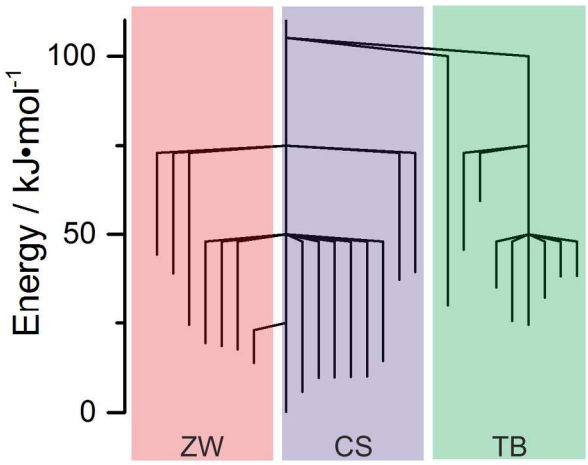

Figure 4. Disconnectivity graph that provides a coarse-grained topological map of the PES of protonated 3-CF_3-Phe•TMA. The bottoms of vertical lines correspond with local minima on the electronic PES. Points where lines intersect correspond to energies above which minima can interconvert. Minima highlighted in red (left) correspond with zwitterion isomers (ZW), in blue (centre) correspond with canonical isomers (CS), and in green (right) correspond with TMA−bridged isomers (TB). Calculations employed the B3LYP functional and 6-311++G(d,p) basis set.

In examining the fine details of the PES, we find that the lowest energy barriers to structural interconversion are associated with rotation of the trifluoromethyl group and the TMA moiety about its hydrogen bond axis. Rotamer interconversion typically requires less than *ca.* 11 kJ•mol^{-1}. Isomerization via proton transfer typically occurs in the energy range of 20–30 kJ•mol^{-1} above the global minimum. The lowest energy pathway to access zwitterion structures from the canonical motif is intramolecular proton-transfer from the OH group of global minimum to the amine, thus producing isomer 7 (see figure 2). The barrier to interconversion between the global minimum and isomer 7 is $E_{electronic}$ = 20.5 kJ•mol^{-1} (see supporting information for various thermodynamic corrections). At energies above $E_{electronic}$ ≈ 28 kJ•mol^{-1}, conformational changes can occur in canonical isomers via rotation about the dihedral angles associated with the saturated carbon chain of the phenylalanine moiety. Zwitterion species, like the canonical structures, can also interconvert via rotation about the dihedral angles of the carbon chain. Isomerization barriers for zwitterion dihedral rotation are typically *ca.* 40 kJ•mol^{-1} above the global minimum. However, the most energetically favourable pathways for zwitterion conformer interconversion involve proton transfer to yield a canonical structure, followed by dihedral isomerization of the canonical conformer and subsequent proton transfer to generate a different zwitterion isomer. Isomerization barriers along the proton-transfer / dihedral rotation / proton-transfer pathways are *ca.* 30 kJ•mol^{-1} above the global minimum.

At energies in excess of *ca.* 65 kJ•mol^{-1} above the global minimum, dihedral rotation about the carbon-carbon bond of the amino acid group can occur. Isomerization via this pathway results in high energy structures (*e.g.*, TMA•H^+ interacting with the OH group) for which we see no evidence in the IRMPD spectra. The highest energy transition state identified (shown in figure 5) is 104.6 kJ•mol^{-1} ($\Delta G°$ = 96.9 kJ•mol^{-1}) above the global minimum and it is associated with dihedral rotation about the amino acid carbon-carbon bond in a TMA-bridged structure. To investigate which minima are connected by this transition state, the transition state structure was distorted along the unbound normal mode and subsequently geometry optimized. This treatment resulted in the production of a TMA−bridged isomer for one displacement direction, but did not yield a second stable minimum in the opposite direction. The fact that a second minimum was not found can be rationalized based on the transition state's geometry and energy. The displacement vectors associated with this transition state show that cluster energy is lowered by rotating the COOH group so as to move the acidic hydrogen away from the TMA•H^+•••NH_2 region (see figure 5). Rotating the COOH group in the opposite direction (clockwise as plotted in figure 5) would improve the intramolecular alignment for proton-sharing between the amine and carboxylic acid

groups, however, such a structure is likely unstable owing to the proximity of the charge-carrying proton on the TMA•H$^+$ with the acidic hydrogen of the carboxylic acid. Indeed, a potential energy scan along the unbound normal mode coordinate of the 104.6 kJ•mol^{-1} transition state shows a broad, shallow (*ca*. 8 cm^{-1}) minimum wherein the N−C−C−O dihedral angle has been reduced from 43.5° (at the transition state) to 34.6°. No transition state connecting the TMA-bridged structures to the canonical or zwitterion structures was found. One could envision a pathway whereby an N-bound TMA-bridged structure isomerizes to an O-bound TMA-bridged structure (*e.g.*, isomer 15, Supporting Information), followed by an amino acid dihedral rotation. However, this would likely occur at an energy in excess of the 104.6 kJ•mol^{-1} transition state and the dissociation threshold for TMA + zwitterion 3-CF$_3$-Phe•H$^+$ production (*vide infra*). Thus, the implication of the 104.6 kJ•mol^{-1} transition state and the apparent isomerization pathway is that TMA−bridged isomers are associated with a deep secondary funnel on the cluster PES (as shown in figure 4). Owing to this feature of the 3-CF$_3$-Phe•TMA•H$^+$ potential energy landscape, TMA−bridged structures become kinetically trapped upon formation.

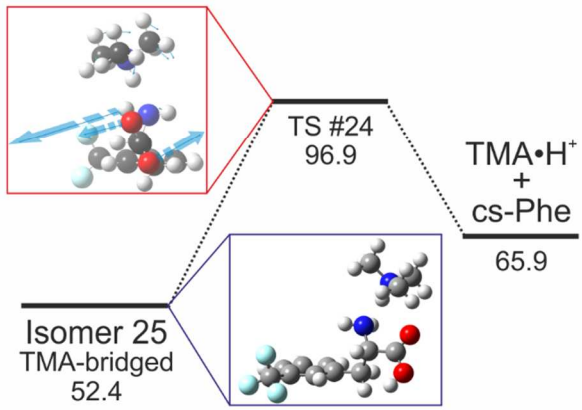

Figure 5. A high energy transition state of 3-CF$_3$-Phe•TMA•H$^+$ that results in production of a TMA−bridged isomer. Standard Gibb's energies (relative to the ground state) are given in kJ•mol^{-1}. Calculations were conducted at the B3LYP/ 6-311++G(d,p) level of theory.

Cluster Fragmentation

IRMPD of charge-solvated clusters results in fragmentation exclusively via production of TMA•H$^+$. The explanation as to why this is the case becomes clear if we consider the relative standard Gibb's free energies along the dissociation pathway. Figure 6 shows the energetics of this process as calculated at the DFT and MP2 levels of theory. The threshold for production of TMA•H$^+$ and charge-solvated 3-CF$_3$-Phe lies $\Delta G°$ = 65.9 kJ•mol^{-1} above the global minimum. Thus, four photons of *ca*. 1750 cm^{-1} are required to induce dissociation from the global minimum isomer. To produce TMA and O-protonated 3-CF$_3$-Phe•H$^+$ (*i.e.*, protonation of the canonical structure on the carbonyl), $\Delta G°$ = 258.6 kJ•mol^{-1} must be overcome, which requires 13 photons of *ca*. 1750 cm^{-1}. This is more than three times the photon requirement for TMA•H$^+$ production and it is highly unlikely that the parent cluster would remain intact to absorb the 13th photon given a statistical sampling of the available states at the 4- to 12-photon levels. The relatively high energy of this product threshold arises due to the relative instability of the O-protonated 3-CF$_3$-Phe•H$^+$ structure (where both oxygen atoms are bound to a hydrogen atom). An alternate route to TMA production involves formation of a N-protonated 3-CF$_3$-Phe•H$^+$ co-fragment (*i.e.*, protonation of the canonical structure on the amine). This threshold lies $\Delta G°$ = 109.8 kJ•mol^{-1} above the canonical global minimum. However, accessing the TMA + N-protonated 3-CF$_3$-Phe•H$^+$ dissociation threshold from the canonical structures requires isomerization to a zwitterion cluster isomer *en route*. Such an isomerization would render the cluster transparent to subsequent photo-excitation via the distinct charge-solvated C=O stretch normal mode.

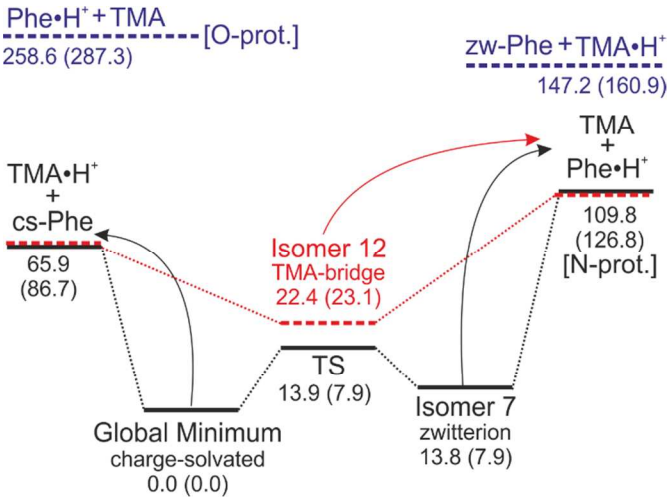

Figure 6. Relative standard Gibbs free energies along the dissociation pathways of protonated 3-CF$_3$-Phe•TMA as calculated at the B3LYP/6-311G++(d,p) level of theory at 298 K. Values in parentheses give the free energies with electronic contributions calculated at the MP2/*aug*-cc-pVTZ level of theory. Energies are reported in kJ•mol^{-1}. Charge-solvated and zwitterionic phenylalanine derivatives are represented by cs/zw-Phe. Arrows indicate which product channel threshold is accessed by excitation of the carbonyl stretching mode.

Zwitterion isomers were found to dissociate exclusively via a TMA + 3-CF$_3$-Phe•H$^+$ product channel when exciting their C=O stretching modes. The lowest energy dissociation threshold for production of these species is the TMA + N-protonated 3-CF$_3$-Phe•H$^+$ channel, which can be accessed from the lowest energy zwitterion cluster with five photons of *ca*. 1750 cm^{-1}. To produce O-protonated 3-CF$_3$-Phe•H$^+$ requires an additional seven *ca.* 1750 cm^{-1} photons (*i.e.*, 12 photons in total). Thus, production of N-protonated 3-CF$_3$-Phe•H$^+$ is clearly favored energetically.

The fact that TMA•H$^+$ production is not observed for zwitterion cluster IRMPD might seem surprising based on the calculated cluster dissociation thresholds. Given that the TMA•H$^+$ + canonical 3-CF$_3$-Phe product channel can be

reached with only three 1750 cm^{-1} photons from the lowest energy zwitterion cluster (compared to five photons for the TMA + N-protonated 3-CF_3-Phe•H^+ channel), one might expect that production of TMA•H^+ should be the dominant fragmentation pathway. The fact that this does not occur provides some qualitative insight into the IRMPD dynamics for the zwitterion clusters. If, following photon absorption, zwitterion clusters isomerize to canonical cluster structures, these isomers become transparent to further excitation via the zwitterion C=O stretch wavenumber and would not be observed in IRMPD. Therefore, while isomerization may occur at the one or two photon level, it has no bearing on the observed photofragmentation. However, should isomerization occur at the three or four photon level, the result would likely be fragmentation to yield TMA•H^+ + canonical 3-CF_3-Phe. The fact that this pathway is not observed therefore suggests that the rate for isomerization and dissociation to form TMA•H^+ is lower than the rate for photon absorption and dissociation to form N-protonated 3-CF_3-Phe•H^+ at the 3- and 4-photon levels for our experimental conditions.

TMA−bridged cluster isomers are also found to exclusively access the TMA + 3-CF_3-Phe•H^+ product channel when excited via their C=O stretching mode. The lowest energy TMA + N-protonated 3-CF_3-Phe•H^+ channel can be accessed from the lowest energy TMA−bridged cluster with five photons of *ca*. 1750 cm^{-1}. Dissociation via the lowest energy TMA + O-protonated 3-CF_3-Phe•H^+ channel requires at least 12 *ca*. 1750 cm^{-1} photons, and is therefore unlikely to occur via IRMPD. The threshold for production of TMA•H^+ + canonical 3-CF_3-Phe occurs only $\Delta G°$ = 43.5 kJ•mol^{-1} above the lowest energy TMA−bridged isomer. Thus, only three *ca*. 1750 cm^{-1} photons are required to access the TMA•H^+ production channel. The fact that this product channel is not observed experimentally implies that the dynamics of the dissociation process preclude formation of TMA•H^+ + charge-solvated 3-CF_3-Phe. This can be rationalized by closer consideration of the geometries of the TMA−bridged structures. For example, figure 3 shows the lowest energy TMA−bridged isomer, where it can be seen that the TMA•H^+ moiety is oriented in a bridging fashion to the amine and carbonyl groups, with the proton aligned to interact with the NH_2 lone pair. A direct, impulsive dissociation mechanism would induce fragmentation along the N−H^+−N axis. Should the TMA•H^+ proton be transferred to the phenylalanine derivative, the TMA fragment would be ejected into a repulsive region of the PES that is associated with interaction between the TMA lone pair electron density and that of the carbonyl oxygen atom. This dissociation process results in production of TMA and the lowest energy N-protonated 3-CF_3-Phe•H^+ isomer ($\Delta G°$ = 109.8 kJ•mol^{-1} above the global minimum). This mechanism is consistent with the IRMPD observations. If, on the other hand, the TMA moiety retains the proton in the impulsive model, the TMA•H^+ is driven into an attractive region of the PES that is associated with interaction between the proton and lone pair electron density of the carbonyl oxygen atom. Indeed, isomer 15 (30.2 kJ•mol^{-1}) is a high-energy TMA−bridged structure wherein the TMA•H^+ moiety is instead oriented such that the proton is aligned to interact with the carbonyl oxygen. Interaction between TMA•H^+ moiety and the carbonyl group results in a significant shift in the C=O stretch vibrational peak (*ca*. 85 cm^{-1} to lower wavenumber). This renders the TMA−bridged cluster transparent to subsequent excitation via the C=O vibrational band that is specific to the nitrogen-oriented TMA−bridged structures, essentially blocking dissociation via the lower energy TMA•H^+ + canonical 3-CF_3-Phe product channel.

As was the case with excitation via the C=O stretch, the COH bending mode of the canonical species (1418 cm^{-1}), also produces TMA•H^+ exclusively. This can be rationalized using similar logic to that employed for the higher wavenumber regions – should isomerization occur during IRMPD, the new zwitterion structure will be transparent to excitation at that particular wavenumber. The same seems to be true of the feature at 1350 cm^{-1}, which appears clearly in the TMA•H^+ channel, but which is only (at best) a minor contribution to the breadth of the 1332 cm^{-1} peak in the 3-CF_3-Phe•H^+ channel. Interestingly, both product channels exhibit similar spectra below 1350 cm^{-1}. This occurs due to fortuitous overlap of the spectra for the three structural motifs – all three families of isomers exhibit vibrational transitions at *ca*. 1330 cm^{-1}, *ca*. 1235 cm^{-1}, and *ca*. 1210 cm^{-1}. The slight relative enhancement of the *m/z* = 234 compared to the *m/z* = 60 channel in the 1200 – 1250 cm^{-1} region is likely due to IRMPD of the TMA-bridged structures, which produces a minor amount of 3-CF_3-Phe•H^+ across the entire spectral range (based on our computational study).

Comparison with 3-CN-Phe•TMA•H^+

Although both 3-CF_3-Phe•TMA•H^+ and 3-CN-Phe•TMA•H^+ yield the same IRMPD products, x-Phe•H^+ (where x = CN, CF_3) and TMA•H^+, it is noteworthy that the canonical, zwitterion, and TMA-bridged structural motifs do not similarly access these product channels in the two cluster derivatives. For example, the TMA-bridged structures of 3-CN-Phe•TMA•H^+ access the TMA•H^+ and 3-CN-Phe•H^+ product channels with near equal probability, whereas the TMA-bridged structures of 3-CF_3-Phe•TMA•H^+ only yield 3-CF_3-Phe•H^+ upon IRMPD (see table 1).[9] In the case of the cyano derivative, the two different IRMPD mass channels exhibited different spectra across the entire 1000 – 2000 cm^{-1} range. Consequently, it was very clear that canonical structures dissociated exclusively via the TMA•H^+ product channel, and that zwitterion structures dissociated exclusively via the 3-CN-Phe•H^+ product channel.[9] The same is true for the trifluoromethyl derivative, but only at wavenumbers greater than *ca*. 1350 cm^{-1}; at $\bar{\nu}$ < 1350 cm^{-1}, the IRMPD spectra are nearly identical in both product channels.

The fact that the canonical and zwitterion motifs of 3-CF_3-Phe•TMA•H^+ exhibit nearly identical spectra in the 1200 – 1250 cm^{-1} region has interesting implications with respect to IRMPD. On first glance, one might consider the near equal peak intensities in this region to be indicative of near equal

populations of zwitterion and canonical structures and that, based on comparison with the cyano derivative, zwitterions should fragment to yield 3-CF_3-Phe•H^+, while canonical structures should produce TMA•H^+. However, the IRMPD process relies on the fact that the rate of intramolecular vibrational redistribution (IVR) is significantly fast such that absorbed photon energy is statistically distributed amongst cluster bath states prior to absorption of subsequent photons. For canonical structures this can result in isomerization to the analogous zwitterion (and vice versa). Isomer specific IRMPD for these species relies on the fact that isomerization renders a particular species transparent to photon absorption at the fixed wavelength of the FEL. However, if two isomers have near-resonant absorptions (as is the case in the 1200 – 1250 cm^{-1} region for 3-CF_3-Phe•TMA•H^+), the newly formed isomer can continue absorbing IR energy to induce fragmentation following photo-induced isomerization. Thus, canonical and zwitterion clusters of 3-CF_3-Phe•TMA•H^+ exhibit vibrational mode-selective chemistry; at wavenumbers greater than 1350 cm^{-1} they exclusively access one product channel owing to deactivation of other product channels by IR-induced isomerization/transparency, while excitation in the 1200 – 1250 cm^{-1} range (likely) yields both product channels owing to the fortuitous overlap of vibrational modes for zwitterion and canonical structural motifs. This possibility could be unambiguously tested by selecting specific isomers with ion chromatographic techniques (e.g., DMS, FAIMS) prior to conducting IRMPD.[41-45]

Table 1. A summary of the observed IRMPD channels for protonated 3-x-Phe•TMA (x = CF_3, CN).[9]

x-Phe•TMA•H^+	→ x-Phe + TMA•H^+	[Channel I]
	→ x-Phe •H^+ + TMA	[Channel II]

Motif	1000 – 1350 cm^{-1}		1350 – 1900 cm^{-1}	
	CN	CF_3	CN	CF_3
Canonical	I	I & II	I	I
Zwitterion	II	I & II	II	II
TMA-bridged	I & II	II	I & II	II

Conclusions

IRMPD of 3-CF_3-Phe•TMA•H^+ results in production of TMA•H^+ (*m/z* = 60) and 3-CF_3-Phe•H^+ (*m/z* = 234). In the 1000 – 1350 cm^{-1} region of the spectrum, both product channels exhibit similar spectra, whereas at $\bar{\nu} >$ 1350 cm^{-1} the spectra observed in the two product channels are dramatically different. A thorough search of the cluster potential energy landscape identified three structural motifs: (1) canonical, (2) zwitterion, and (3) TMA-bridged. TMA-bridged isomers are high energy, metastable structures which are kinetically trapped during cluster formation, and which are not accessible from the canonical/zwitterion region of the PES. TMA-bridged structures fragment *exclusively* via the TMA + N-protonated 3-CF_3-Phe•H^+ product channel across the entire spectral range.

In the 1350 – 2000 cm^{-1} region, canonical structures are observed to fragment *exclusively* via the TMA•H^+ + canonical 3-CF_3-Phe product channel. Zwitterion structures, on the other hand, fragment *exclusively* via the TMA + N-protonated 3-CF_3-Phe•H^+ product channel in this region. To access the other threshold, each of these structural motifs must isomerize during the IRMPD process. However, clusters that do isomerize are rendered transparent to subsequent IR photo-excitation owing to the fact that their vibrational transitions are no longer resonant with the FEL. This effectively deactivates one of the two product channels. In the 1000 – 1350 cm^{-1} region, on the other hand, the canonical and zwitterion structures exhibit similar spectra. Here, a canonical cluster that isomerizes during photo-excitation can continue to absorb IR energy via near-resonant transition associated with the zwitterion structure (and vice versa). Thus, the canonical and zwitterionic motifs can access both the TMA•H^+ and 3-CF_3-Phe•H^+ product channels in this spectral region, and apparently do so with nearly equal probability. Note that the process described here is subtly different from the traditional view of mode-selective chemistry where, for processes with similar internal energy content, the reaction outcome is controlled by the mode of internal excitation.[17]

The isomer-specific and mode-selective control of the IRMPD dissociation process for 3-CF_3-Phe•TMA•H^+ arises due to the shape of the cluster potential energy landscape. In other similar clusters (*e.g.*, 3-CN-Phe•TMA•H^+), isomer-specificity was observed in IRMPD, but not mode-selectivity.[9, 12-17] This suggests that mode-selectivity in amino acid-containing clusters might be tuneable based on the substitution scheme of the side chain since this provides a subtle tuning of the PES (and, therefore, vibrational frequencies). Consequently, the combination of side-chain chemical substitution and mode-specific vibrational excitation might provide exquisite control over amino acid chemistry. Whether the potential for mode-selective chemistry in the case of 3-CF_3-Phe•TMA•H^+ is unique and fortuitous amongst amino acid clusters, or instead hints at this being a general feature of the photochemistry associated with these species is currently an open question.

Acknowledgements

We gratefully acknowledge high performance computing support from the SHARCNET consortium of Compute Canada. We are also grateful to the Centre Laser Infrarouge d'Orsay (CLIO) team and technical support staff for the valuable assistance and hospitality. The authors would like to acknowledge financial support from the Natural Sciences and Engineering Research Council (NSERC) of Canada.

Notes and references

*Scott Hopkins: shopkins@uwaterloo.ca
**Terry McMahon: mcmahon@uwaterloo.ca

1. Department of Chemistry, University of Waterloo, Waterloo, ON, Canada, N2L 3G1.

2. Laboratoire Chimie Physique – CLIO, Bâtiment 201, Porte 2, Campus Universitaire d'Orsay, Orsay, France, 91405

Electronic Supplementary Information (ESI) available: Cluster structures, XYZ coordinates, energies, and vibrational spectra are provided. See DOI: 10.1039/b000000x/

1. M. F. Bush, J. S. Prell, R. J. Saykally and E. R. Williams, *Journal of the American Chemical Society*, 2007, 129, 13544-13553.
2. C. J. Chapo, J. B. Paul, R. A. Provencal, K. Roth and R. J. Saykally, *Journal of the American Chemical Society*, 1998, 120, 12956-12957.
3. R. R. Julian, R. Hodyss and J. L. Beauchamp, *Journal of the American Chemical Society*, 2001, 123, 3577-3583.
4. C. Kapota, J. Lemaire, P. Maitre and G. Ohanessian, *Journal of the American Chemical Society*, 2004, 126, 1836-1842.
5. A. Lesarri, E. J. Cocinero, J. C. Lopez and J. L. Alonso, *Angewandte Chemie-International Edition*, 2004, 43, 605-610.
6. R. Wu and T. B. McMahon, *Angewandte Chemie-International Edition*, 2007, 46, 3668-3671.
7. R. Wu and T. B. McMahon, *Journal of Mass Spectrometry*, 2008, 43, 1641-1648.
8. T. Wyttenbach, M. Witt and M. T. Bowers, *Journal of the American Chemical Society*, 2000, 122, 3458-3464.
9. W. S. Hopkins, R. A. Marta and T. B. McMahon, *Journal of Physical Chemistry A*, 2013, 117, 10714-10718.
10. E. P. Hunter and S. G. Lias, *J. Phys. Chem. Ref. Data*, 1998, 27, 413-656.
11. R. S. Ruoff, T. D. Klots, T. Emilsson and H. S. Gutowsky, *J. Chem. Phys.*, 1990, 93, 3142-3150.
12. R. B. Metz, J. D. Thoemke, J. M. Pfeiffer and F. F. Crim, *J. Chem. Phys.*, 1993, 99, 1744-1751.
13. J. C. Polanyi, *Accounts Chem. Res.*, 1972, 5, 161-&.
14. A. Sinha, M. C. Hsiao and F. F. Crim, *J. Chem. Phys.*, 1991, 94, 4928-4935.
15. A. Sinha, R. L. Vanderwal and F. F. Crim, *J. Chem. Phys.*, 1990, 92, 401-410.
16. S. Yan, Y. T. Wu, B. L. Zhang, X. F. Yue and K. P. Liu, *Science*, 2007, 316, 1723-1726.
17. R. N. Zare, *Science*, 1998, 279, 1875-1879.
18. J. M. Ortega, F. Glotin and R. Prazeres, *Infrared Physics & Technology*, 2006, 49, 133-138.
19. W. S. Hopkins, M. Hasan, M. Burt, R. A. Marta, E. Fillion and T. B. McMahon, *Journal of Physical Chemistry A*, 2014, 118, 3795-3803.
20. J. K. Martens, I. Compagnon, E. Nicol, T. B. McMahon, C. Clavaguera and G. Ohanessian, *Journal of Physical Chemistry Letters*, 2012, 3, 3320-3324.
21. R. Wu, R. A. Marta, J. K. Martens, K. R. Eldridge and T. B. McMahon, *Journal of the American Society for Mass Spectrometry*, 2011, 22, 1651-1659.
22. B. E. Ziegler, R. A. Marta, S. M. Martens, J. K. Martens and T. B. McMahon, *International Journal of Mass Spectrometry*, 2012, 316, 117-125.
23. M. J. Frisch, G. W. Trucks, H. B. Schlegel, G. E. Scuseria, M. A. Robb, J. R. Cheeseman, G. Scalmani, V. Barone, B. Mennucci, G. A. Petersson and e. al., in *Gaussian, Inc. Wallingford CT* 2009.
24. M. J. Lecours, W. C. T. Chow and W. S. Hopkins, *Journal of Physical Chemistry A*, 2014, 118, 4278-4287.
25. A. D. Becke, *Physical Review A*, 1988, 38, 3098-3100.
26. C. T. Lee, W. T. Yang and R. G. Parr, *Physical Review B*, 1988, 37, 785-789.
27. B. Miehlich, A. Savin, H. Stoll and H. Preuss, *Chemical Physics Letters*, 1989, 157, 200-206.
28. J. J. P. Stewart, *Journal of Molecular Modeling*, 2007, 13, 1173-1213.
29. C. Y. Peng, P. Y. Ayala, H. B. Schlegel and M. J. Frisch, *Journal of Computational Chemistry*, 1996, 17, 49-56.
30. C. Y. Peng and H. B. Schlegel, *Israel Journal of Chemistry*, 1993, 33, 449-454.
31. P. Parneix, M. Basire and F. Calvo, *Journal of Physical Chemistry A*, 2013, 117, 3954-3959.
32. K. T. Crampton, A. I. Rathur, Y. W. Nei, G. Berden, J. Oomens and M. T. Rodgers, *Journal of the American Society for Mass Spectrometry*, 2012, 23, 1469-1478.
33. R. C. Dunbar, J. D. Steill and J. Oomens, *Journal of the American Chemical Society*, 2011, 133, 1212-1215.
34. S. M. Martens, R. A. Marta, J. K. Martens and T. B. McMahon, *Journal of Physical Chemistry A*, 2011, 115, 9837-9844.
35. S. M. Martens, R. A. Marta, J. K. Martens and T. B. McMahon, *J. Am. Soc. Mass Spectrom.*, 2012, 23, 1697-1706.
36. R. J. Nieckarz, J. Oomens, G. Berden, P. Sagulenko and R. Zenobi, *Physical Chemistry Chemical Physics*, 2013, 15, 5049-5056.
37. D. J. Wales and J. P. K. Doye, *Journal of Physical Chemistry A*, 1997, 101, 5111-5116.
38. M. Burt, K. Wilson, R. Marta, M. Hasan, W. S. Hopkins and T. McMahon, *Physical Chemistry Chemical Physics*, 2014, 16, 24223-24234.
39. D. J. Wales, *Energy Landscapes with Applications to Clusters, Biomolecules and Glasses*, Cambridge University Press, Cambridge, 2003.
40. L. Mac Aleese, A. Simon, T. B. McMahon, J. M. Ortega, D. Scuderi, J. Lemaire and P. Maitre, *International Journal of Mass Spectrometry*, 2006, 249, 14-20.
41. D. A. Barnett, B. Ells, R. Guevremont and R. W. Purves, *Journal of the American Society for Mass Spectrometry*, 1999, 10, 1279-1284.
42. J. L. Campbell, M. Zhu and W. S. Hopkins, *Journal of the American Society for Mass Spectrometry*, 2014, 25, 1583-1591.
43. E. V. Krylov and E. G. Nazarov, *International Journal of Mass Spectrometry*, 2009, 285, 149-156.
44. E. V. Krylov, E. G. Nazarov and R. A. Miller, *International Journal of Mass Spectrometry*, 2007, 266, 76-85.
45. W. S. Hopkins, *Molecular Physics*, 2015, DOI: 10.1080/00268976.2015.1053545, 1-8.

